

# Instantaneous-Shape Sampling for Calculation of the Electromagnetic Dipole Strength in Transitional Nuclei

S. Q. Zhang <sup>\*,1</sup> I. Bentley,<sup>2</sup> S. Brant,<sup>3</sup> F. Dönau,<sup>1</sup> S. Frauendorf,<sup>1,2</sup> B. Kämpfer,<sup>1</sup> R. Schwengner,<sup>1</sup> and A. Wagner<sup>1</sup>

<sup>1</sup>*Institut für Strahlenphysik, Forschungszentrum Dresden-Rossendorf, 01314 Dresden, Germany*

<sup>2</sup>*Department of Physics, University of Notre Dame, Notre Dame, IN 46556, USA*

<sup>3</sup>*Department of Physics, Faculty of Science, University of Zagreb, 10000 Zagreb, Croatia*

(Dated: November 2, 2018)

Electromagnetic dipole absorption cross-sections of transitional nuclei with large-amplitude shape fluctuations are calculated in a microscopic way by introducing the concept of Instantaneous Shape Sampling. The concept bases on the slow shape dynamics as compared to the fast dipole vibrations. The electromagnetic dipole strength is calculated by means of RPA for the instantaneous shapes, the probability of which is obtained by means of IBA. Very good agreement with the experimental absorption cross sections near the nucleon emission threshold is obtained.

PACS numbers: 21.60.Fw, 21.60.Jz, 23.20.Lv, 25.20.Dc, 27.60.+j

Photo-nuclear processes, as the absorption of a photon inducing the emission of a neutron or the emission of a photon after neutron absorption, are key elements in various astrophysical scenarios, like supernovae explosions or  $\gamma$ -ray bursts, as well as in simulations for nuclear technology. For a quantitative description of the relevant nuclear reactions one needs to know the  $\gamma$ -absorption cross section and the reemission probability, being determined by the dipole strength function. Direct measurements of the strength function in the relevant energy range (typically 6-10 MeV in medium-heavy nuclei) are not possible nowadays for most of the unstable nuclei passed in violent stellar events. Theoretical models that provide reliable prediction of the dipole strength function are therefore of utter importance. Aside from the astrophysical applications understanding the mechanisms that determine the structure of the dipole strength function in this energy region is a challenge of its own to nuclear theory. The present Letter proposes and tests a new approach, which we call Instantaneous Shape Sampling (ISS). It combines the microscopic Random Phase Approximation (RPA) for dipole excitations with the phenomenological Interacting Boson Approximation (IBA) for a dynamical treatment of the nuclear shape. ISS allows one to calculate the dipole strength function of the many transitional nuclei ranging between the regions of spherical and well deformed shape.

Traditionally one employs phenomenological expressions for the dipole strength function [1], which are based on the classical model of a damped collective Giant Dipole Resonance (GDR). The photo-absorption cross section  $\sigma_\gamma$  of the GDR is approximated by a Lorentzian curve [2, 3, 4, 5], which may include corrections for nuclear deformation [5]. The damping width of the Lorentzian is treated as a parameter that is adjusted to the experiment. However, the available data have not yet allowed stringent tests of this extrapolation toward the low-energy tail of the GDR [4]. Therefore microscopic approaches that treat at least a substantial part of the

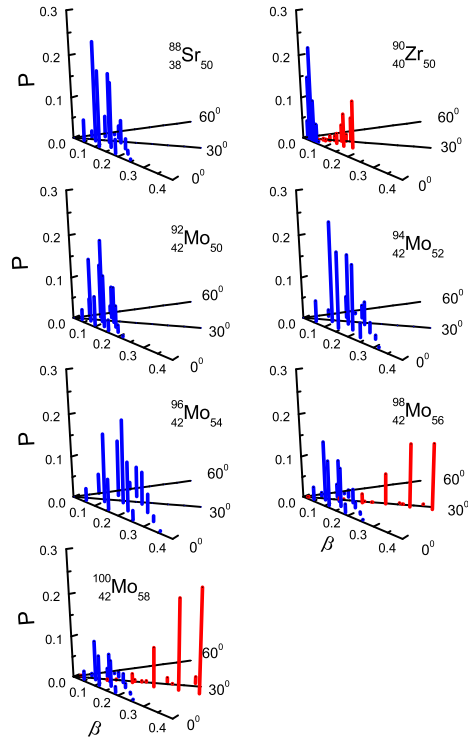


FIG. 1: (Color online) Probability distributions of the instantaneous nuclear shapes over the  $\beta - \gamma$  plane. Families of coexisting shapes are distinguished by their color.

damping explicitly promise improved predictive power.

RPA [6] is the standard microscopic approach to the dipole strength function. It takes the Landau fragmentation into account, which describes the coupling of the collective dipole vibration to the particle-hole excitations. It also describes the splitting of the GDR caused by a static deformation of the mean field. However both effects account only for a fraction of the observed width of the GDR. In order to obtain the experimental damping width of the GDR one must include, at least, the cou-

TABLE I: IBA parameters  $\zeta$ ,  $\chi$ ,  $e_B$ , and equilibrium deformation parameters  $\beta$ ,  $\gamma$  calculated by means of the micro-macro method. In case of shape coexistence, two sets are listed. Their respective proportion in the ground state is given in percentage.

$^A_X$	$\zeta$	$\chi$	$e_B$	%	$\beta$	$\gamma$
$^{88}\text{Sr}$	0.0	-1.20	0.043	100	0.0	0°
$^{90}\text{Zr}$	0.0	-1.20	0.013	64	0.0	0°
	0.60	-0.31	0.040	36		
$^{92}\text{Mo}$	0.25	-1.32	0.040	100	0.0	0°
$^{94}\text{Mo}$	0.29	-1.20	0.064	100	0.02	60°
$^{96}\text{Mo}$	0.20	-1.32	0.069	100	0.10	60°
$^{98}\text{Mo}$	0.0	-1.20	0.053	60	0.18	37°
	0.59	-0.03	0.106	40		
$^{100}\text{Mo}$	0.0	-1.20	0.053	40	0.21	32°
	0.61	-0.10	0.106	60		

pling to the two-particle two-hole states [6]. One may distinguish between two types of such states: the combination of the GDR with incoherent particle-hole excitations and its combination with coherent collective excitations. The coupling to the former is analogue to the collisional damping of Fermi liquids. The latter has been studied for spherical nuclei by means of particle-phonon coupling models, such as QPM [7, 8], QTBA [9], and QRPA-PC [10], which, however, meet principle problems in transitional nuclei.

We suggest an alternative approach. Out of the huge space of collective excitations coupling to the GDR we select only the low-energy collective quadrupole excitations. They represent the softest mode, which couples most strongly to the dipole mode. The coupling, coherently and incoherently, to the other excitations is taken into account by averaging with a Lorentzian of the type that arises from collisional damping [3, 6]. In the following we simply refer to this as “collisional damping” (CD). The typical energies of the quadrupole excitations are below 1 MeV, i.e. about a factor of 10 less than the energy of the dipole excitations. Since the quadrupole motion is ten times slower than the dipole one we use the adiabatic approximation: By means of RPA, we calculate the dipole absorption cross section  $\sigma_\gamma(E, \beta_n, \gamma_n)$  for a set of instantaneous deformation parameters  $\{\beta_n, \gamma_n\}$  of the mean field. We find the probability  $P(\beta_n, \gamma_n)$  of each shape being present in the ground state by means of IBA-1, and obtain the total cross section as the incoherent sum of the instantaneous ones,

$$\sigma_\gamma(E) = \sum_n P(\beta_n, \gamma_n) \sigma_\gamma(E, \beta_n, \gamma_n). \quad (1)$$

In other words, we assume that the quadrupole deformation does not change during the excitation of the nucleus by the absorbed photons, which sample the instantaneous shapes of the nucleus in the ground state. Accordingly we suggest the acronym ISS-RPA for the approach.

Ref. [11] studied a collective dipole vibration coupled to a harmonic quadrupole vibration and showed that the

adiabatic approximation rather well reproduces the exact spreading. The ISS expression (1) is of very general nature. All versions of RPA based on a deformed mean field could be used to calculate  $\sigma_\gamma(E, \beta_n, \gamma_n)$ . Likewise, any model describing the the collective quadrupole mode could be used to obtain  $P(\beta_n, \gamma_n)$ .

We adopt the quasiparticle version of RPA (QRPA) described in [12], which combines a triaxial potential with separable interactions. We changed to a Woods-Saxon potential with “Universal Parameters”. The pairing gaps are adjusted to the even-odd mass differences. The E1-part of  $\sigma_\gamma$  is calculated with an isovector dipole-dipole interaction, the strength of which is adjusted to the experimental position of the maximum of the GDR. The M1-part is calculated with a repulsive isovector spin-spin and an isoscalar quadrupole-quadrupole interaction (for details cf. [13]). The  $\sigma_\gamma(E)$  are calculated using the strength function method with a resolution of 100 keV.

We describe collective quadrupole mode by means of IBA-1 [14], which is known to well reproduce the development of energies and E2-transition probabilities from spherical to well deformed nuclei through the transition region. We use the “extended consistent Q formalism”. The Hamiltonian and the E2-transition operators are given in [15]. The parameters  $\zeta$ ,  $\chi$ ,  $e_B$  of the model are listed in Table I. For practical reasons we fix the boson number to  $N_B = 10$ , which turned out to be a sufficient flexible basis. The probability distribution  $P(\beta_n, \gamma_n)$  is generated by means of the method suggested in [16]. We consider the two scalar operators

$$\hat{q}_2 = [Q^\chi \otimes Q^\chi]_0, \quad (2)$$

$$\hat{q}_3 = [Q^\chi \otimes [Q^\chi \otimes Q^\chi]_2]_0, \quad (3)$$

which are formed by angular momentum coupling from the IBA quadrupole operators  $Q_\mu^\chi$ . The two commuting operators  $\hat{q}_2$  and  $\hat{q}_3$  are diagonalized in the space of states generated by coupling 10 bosons to zero angular momentum. The resulting eigenvalues  $q_{2,n}$  and  $q_{3,n}$  and the eigenstates  $|n\rangle$  are linked to the deformation parameters as follows

$$\beta_n^2 = \sqrt{5} \left( \frac{4\pi e_B}{3ZeR^2} \right)^2 q_{2,n}, \quad \cos 3\gamma_n = \sqrt{\frac{7}{2\sqrt{5}}} \frac{q_{3,n}}{(q_{2,n})^3}. \quad (4)$$

The probabilities  $P(\beta_n, \gamma_n) = |\langle 0_1^+ | n \rangle|^2$  are the projections of the IBA ground state  $|0_1^+\rangle$  on the set  $|n\rangle$ . The method is easily generalized to the case of shape coexistence. In this case one has two families of states,  $a$  and  $b$ . They are described by two sets of IBA parameters and the mixing coefficients  $c_a^2$  and  $c_b^2 = 1 - c_a^2$ , which give the fraction of each family in the ground state. We generate  $P(\beta_{na}, \gamma_{na})$  and  $P(\beta_{nb}, \gamma_{nb})$  separately. The total distribution is then given by  $c_\nu^2 P(\beta_{n\nu}, \gamma_{n\nu})$ ,  $\nu = a, b$ , and the sum in (1) runs over all combinations  $\{n, \nu\}$ .

We applied the method to the nuclides  $^{88}\text{Sr}$ ,  $^{90}\text{Zr}$  and  $^{92-100}\text{Mo}$ , for which the combination of earlier  $(\gamma, n)$

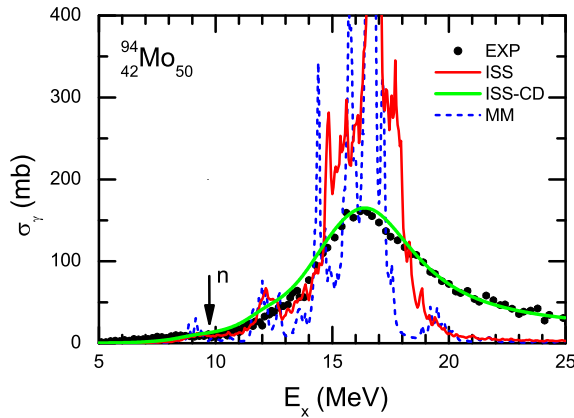


FIG. 2: (Color online) Photo-absorption cross section of  $^{94}\text{Mo}$ . MM: RPA for the equilibrium deformation, ISS: RPA averaged over the probability distributions for shapes in Fig. 1, ISS-CD: ISS folded with a Lorentzian of width  $\alpha E^2$ . Experimental data from [17]

measurements [1] with recent  $(\gamma, \gamma')$  experiments at the ELBE facility [17, 18, 19, 20] provided absorption cross sections  $\sigma_\gamma(E)$  covering the whole energy range from the GDR down to few MeV. The IBA parameters were obtained by fitting the energies and  $B(E2)$  values of the lowest  $0^+$ ,  $2^+$ ,  $4^+$  states taken from the ENSDF data base and from [21, 22]. We set the boson number  $N_B = 10$ , but otherwise followed Refs. [21, 22], where we took the mixing compositions from. Fig. 1 demonstrates that the resulting instantaneous shapes are widely distributed across the  $\beta - \gamma$  plane, which reflects the transitional nature of the considered nuclei. In the cases of  $^{90}\text{Zr}$  and  $^{98,100}\text{Mo}$  the two coexisting families of shapes are clearly recognized (blue and red).

Figs. 2, 3, and 4 compare the results with the experimental data. We include the RPA results for the equilibrium deformations (labelled by MM in the figures) listed in Tab. I, which were calculated by means of the micro-macro method [12, 13]. Let us first consider  $^{94}\text{Mo}_{52}$  shown in Figs. 2, and 3. It has a spherical equilibrium shape, but pronounced transitional character, which is demonstrated by the wide distribution of shapes in Fig. 1. The spherical RPA (MM) shows the expected strong fluctuations of  $\sigma_\gamma$ , reflecting the degeneracy of the spherical single particle levels. The substantial Landau fragmentation generates dipole strength in the threshold region which is of the order of the experimental one. Sampling the different instantaneous shapes (ISS) largely wipes out the strong spikes, because the spherical degeneracy is lifted. It shifts additional strength into the region below 14 MeV, such that  $\sigma_\gamma$  comes close to the data. At the center of the GDR, the ISS peak is broader and lower than the spherical RPA one. However, it is still too narrow and too high because the collisional damping is missing [6]. We include it by folding the ISS cross section with

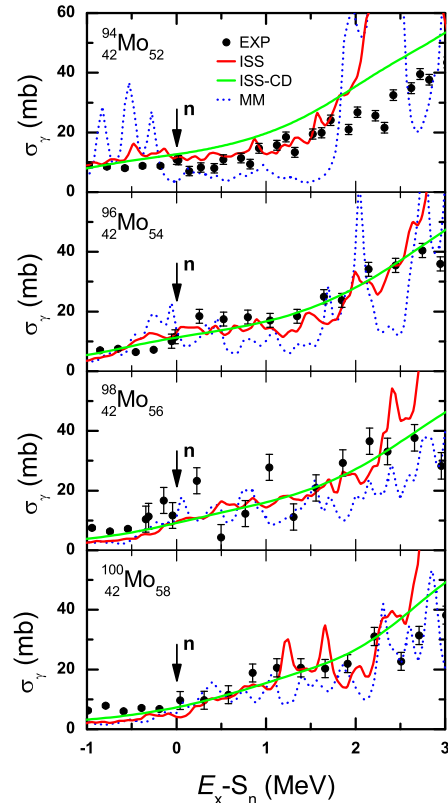


FIG. 3: As Fig. 2 for the energy range around the neutron emission threshold, where  $S_n = 9.68, 9.15, 8.64, 8.29$  MeV for  $N = 52, 54, 56, 58$ , respectively. Data from [17, 18].

a Lorentzian of width  $\Gamma = \alpha E^2$ , which depends on the photon energy as expected for collisional damping [3, 6]. The coefficient  $\alpha$  is chosen to reproduce the experimental  $\sigma_\gamma$  at the maximum of the GDR, which gives  $\alpha = 0.0105$   $\text{MeV}^{-1}$  for the neutron number  $N = 50$  and  $0.014$   $\text{MeV}^{-1}$  for  $N > 50$ . The resulting curve labelled by ISS-CD reproduces the data very well. The agreement of ISS-CD with the data is as good as in Fig. 2 for the other nuclides not shown on this scale.

Figs. 3 and 4 zoom into the region near the nucleon emission thresholds. ISS well describes the experimental  $\sigma_\gamma$  on the average, while still fluctuating too much. The fluctuations are wiped out in the ISS-CD curve, which reproduces the data very well. The inclusion of collisional damping (ISS-CD vs. ISS) hardly shifts additional strength from the GDR to the considered energy region. Hence, the dipole strength near the nucleon emission threshold is determined by the Landau fragmentation of the instantaneous shapes, each of which contributes with its probability being present in the ground state.

In order to quantify the contributions to the width of the GDR peak, we folded the MM and ISS results for  $^{94}\text{Mo}_{52}$  with a Lorentzian of constant width  $\Gamma$ , chosen such that the peak height agreed with the experiment. For the MM case we found  $\Gamma = 4.6$  MeV and

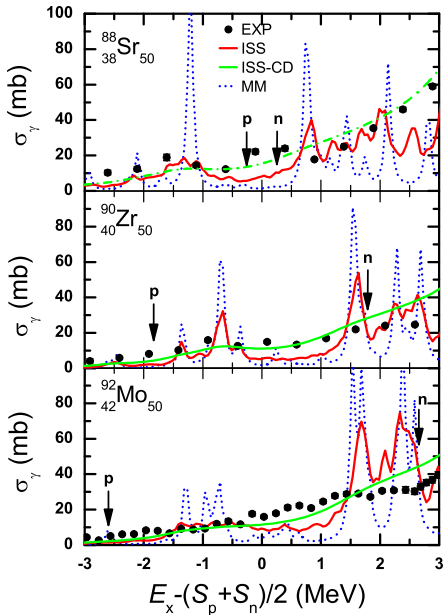


FIG. 4: As Fig. 3. The mean of the proton and neutron thresholds are  $(S_p + S_n)/2 = 10.86, 10.16, 10.06$  MeV for  $Z = 38, 40, 42$ , respectively. Data from [19, 20]

for ISS  $\Gamma=4.0$  MeV. Since the experimental value is  $\Gamma_{exp}=5.7$  MeV, the contribution of the Landau fragmentation is  $\Gamma_{LF}=(5.7-4.6)$  MeV= 1.1MeV. ISS contributes  $\Gamma_{ISS}=(5.7-1.1-4.0)$  MeV=0.6 MeV. The strongest contribution  $\Gamma_{CD}= 4.0$  MeV results from collisional damping. Hence for the “spherical” nucleus  $^{94}\text{Mo}_{52}$  the distribution of dipole strength near the peak of the GDR is dominated by the collisional damping whereas Landau fragmentation and shape fluctuations dominate in the low-energy tail of the GDR. The contribution of shape fluctuations to the peak width increases with  $N$ , going over to the splitting into two peaks characterizing a well deformed shape. Applying the same procedure to the other Mo-isotopes, we found for the collisional damping width  $\Gamma_{CD}=(4.0, 3.6, 3.5, 3.9)$  MeV and for the combined contribution from the fluctuating shape and Landau fragmentation  $\Gamma_{LF+ISS}=(1.7, 2.7, 2.5, 4.0)$  MeV for  $N=94-100$ , respectively.

We reproduce the experimental  $\sigma_\gamma$  near the nucleon emission thresholds using input parameters that are fixed by *independent* information, namely the location of the GDR and low-lying quadrupole excitations. This holds the promise that the concept of ISS-RPA will improve the prediction of the dipole strength for the unstable nuclides passed in the stellar events. We chose the combination, IBA-1 and RPA with dipole-dipole interaction, because it is simple and the modules were available. Our simple RPA can be replaced by more sophisticated versions based on modern density functionals, which are expected to provide reliable dipole strength functions for unstable nuclei. Likewise, the IBA-1 phenomenology can be ex-

tended in a systematic way or it can be replaced by any large-amplitude description for the collective shape degrees of freedom.

In summary, we propose a novel method (ISS-RPA) for calculating the dipole strength function of nuclei with large-amplitude shape fluctuations, which combines the Interacting Boson Model (IBA) with the Random Phase Approximation (RPA). The method bases on the existence of two time scales: the slow shape dynamics and the fast dipole vibrations. Instantaneous Shape Sampling (ISS) assumes that the photo-absorption occurs at a fixed shape, described by RPA, the probability of which given by IBA. We studied the nuclides with  $(Z=38, 40, 42, N=50)$  and  $(Z=42, N=52, 54, 56, 58)$ . ISS-RPA very well reproduces the experimental photo-absorption cross sections  $\sigma_\gamma$ . Around the nucleon emission thresholds,  $\sigma_\gamma$  is determined by the Landau fragmentation and the fluctuating shapes. ISS-RPA may be used for calculating  $\sigma_\gamma$  of unstable nuclei needed in astrophysical simulations of violent stellar events for a firm understanding of the origin of chemical elements in the universe.

This work was supported by the DFG project KA2519/1-1 (Germany) and the US DOE grant DE-FG02-95ER4093.

\* On leave from School of Physics and State-Key Lab. Nucl. Phys. and Tech. Peking University, Beijing 100871, PR China

- [1] <http://www-nds.iaea.org/RIPL-2/>.
- [2] P. Axel, Phys. Rev. **126**, 671 (1962).
- [3] S. G. Kadmenskii *et al.*, Sov. J. Nucl. Phys. **37**, 165 (1983)
- [4] J. Kopecky and M. Uhl, Phys. Rev. C **41**, 1941 (1990).
- [5] T. Rauscher and F.-K. Thielemann, At. Data Nucl. Data Tables **75**, 1 (2000).
- [6] J. Wambach, Rep. Prog. Phys. **51**, 989 (1988).
- [7] V. G. Soloviev, *Theory of Atomic Nuclei: Quasiparticles and Phonons*, Institute of Physics, Bristol, 1992.
- [8] N. Tsoneva and H. Lenske, J. Phys. G **35**, 014047 (2008).
- [9] E. V. Litvinova *et al.*, Phys. Rev. C **78**, 014312 (2008)
- [10] D. Sarti *et al.* Phys. Lett B **601**, 27 (2004) 054318 (2007).
- [11] J. Le Tourneau, Mat. Fys. Medd. Dan. Vid. Selsk. **34**, no 11 (1965), c. f. A. Bohr and B. Mottelson, Nuclear Structure, Vol. II, Benjamin, NY, 1975, p. 455 ff.
- [12] F. Dönau *et al.*, Phys. Rev. C **76**, 014317 (2007).
- [13] G. Rusev *et al.*, Phys. Rev. C **73**, 044308 (2006).
- [14] F. Iachello, A. Arima, The Interacting Boson Model, Cambridge Univ. Press, 1987.
- [15] E. A. McCutchan *et al.*, Phys. Rev. C **69**, 064306 (2004).
- [16] D. Tonev *et al.*, Phys. Rev. C **76**, 044313 (2007).
- [17] A. Wagner *et al.*, J. Phys. G **35**, 014035 (2008).
- [18] G. Rusev *et al.*, Phys. Rev. C **77**, 064321 (2008).
- [19] R. Schwengner *et al.*, Phys. Rev. C **76**, 034321 (2007).
- [20] R. Schwengner *et al.*, Proceedings of Science PoS(PSF07)020, 2008.
- [21] P. E. Garrett *et al.*, Phys. Rev. C **68**, 024312 (2003).
- [22] G. Cata *et al.*, Z. Phys. A **335**, 271 (1990).